nature chemistry

Review article

https://doi.org/10.1038/s41557-026-02113-w

# Tacticity-independent crystallization of polymers

Received: 12 February 2025

Accepted: 19 February 2026

Published online: 3 April 2026

Check for updates

Leire Sangroniz[1], Ainara Sangroniz[1], Changxia Shi[2,3], Miriam Scoti[4], Marta Ximenis[1], Claudio De Rosa[4] ✉, Eugene Y.-X. Chen[2] ✉, Haritz Sardon[1] ✉ & Alejandro J. Müller[1,5] ✉

Crystallization, a phase transition that is prevalent in nature, provides unique molecular arrangements that impact the structure-dependent properties of a material. Owing to thermodynamic and kinetic factors, synthetic polymeric materials show only partial ordering. Indeed, usually polymers that possess sufficient stereo- and regioregularity can partially crystallize. Atactic polymers that do not meet the minimum regularity in the chemical structure needed to pack chains within a crystal unit cell are completely amorphous. However, there are unusual cases where stereoirregular, atactic polymers can crystallize; this happens when the structural features of the atactic polymers provide specific ordering so that their irregular chains can pack into crystalline structures. This Review not only highlights the general relationship between the structures required in atactic polymers to induce crystallization but also provides researchers with the tools to design polymer systems with crystallinity without requiring exquisite stereocontrol in their synthesis.

Crystallization is the most fundamental thermodynamic phase transition in the condensed matter physics of pure substances, and it is prevalent in nature. The most simple and basic crystallization in nature occurs in inorganic materials. Both metals and ceramics can undergo full crystallization. When metals solidify, highly symmetric and dense crystalline structures form due to the non-directional metallic bonding between atoms that allows minimal restrictions in the number and position of nearest-neighbour atoms (Fig. 1a)[1]. Compared with inorganic materials that are composed of atoms and elemental ions, the building blocks of soft materials are typically anisotropic, and conformational heterogeneity plays a critical role in crystallization. The crystallization of soft materials is found in nature, and plays a pivotal role in several biological structures: chitins that protect delicate organisms, proteins that maintain their native configurations through β-folding, DNA that is efficiently packed into chromosomes (Fig. 1b) and celluloses that provide structural support to trees (Fig. 1c); thus, nature can generate ordered structures from disorder, forming highly complex systems[2–4].

Seventy-five per cent of all commercial polymers have a certain degree of crystallinity, which contributes to their desired function, making understanding crystallinity important in human-made materials[5,6]. The presence of crystalline domains improves a polymer's physical and thermomechanical properties[7,8], slows down polymer degradation and increases the barriers to gas and vapour permeation as crystalline domains are impermeable to penetrants[9,10]. Unlike metals or ceramics, polymers have a unique characteristic of being only partially crystalline, that is, semicrystalline (Box 1 and Fig. 1d). Their long-chain structure prevents complete crystallization due to kinetic reasons[11]. The crystallization of polymers requires chain flexibility, high regio- and stereoregularity, and symmetry[12–15]. High regularity and symmetry are easily achieved in linear polymers (without any substituents along the chain) with a flexible main backbone

[1]POLYMAT and Department of Polymers and Advanced Materials: Physics, Chemistry and Technology, Faculty of Chemistry, University of the Basque Country UPV/EHU, Donostia-San Sebastián, Spain. [2]Department of Chemistry, Colorado State University, Fort Collins, CO, USA. [3]Beijing National Laboratory for Molecular Sciences, Laboratory of Polymer Physics and Chemistry, Institute of Chemistry, Chinese Academy of Sciences, Beijing, China. [4]Dipartimento di Scienze Chimiche, Università di Napoli Federico II, Naples, Italy. [5]IKERBASQUE, Basque Foundation for Science, Bilbao, Spain. ✉e-mail: claudio.derosa@unina.it; eugene.chen@colostate.edu; haritz.sardon@ehu.es; alejandrojesus.muller@ehu.es

https://doi.org/10.1038/s41557-026-02113-w

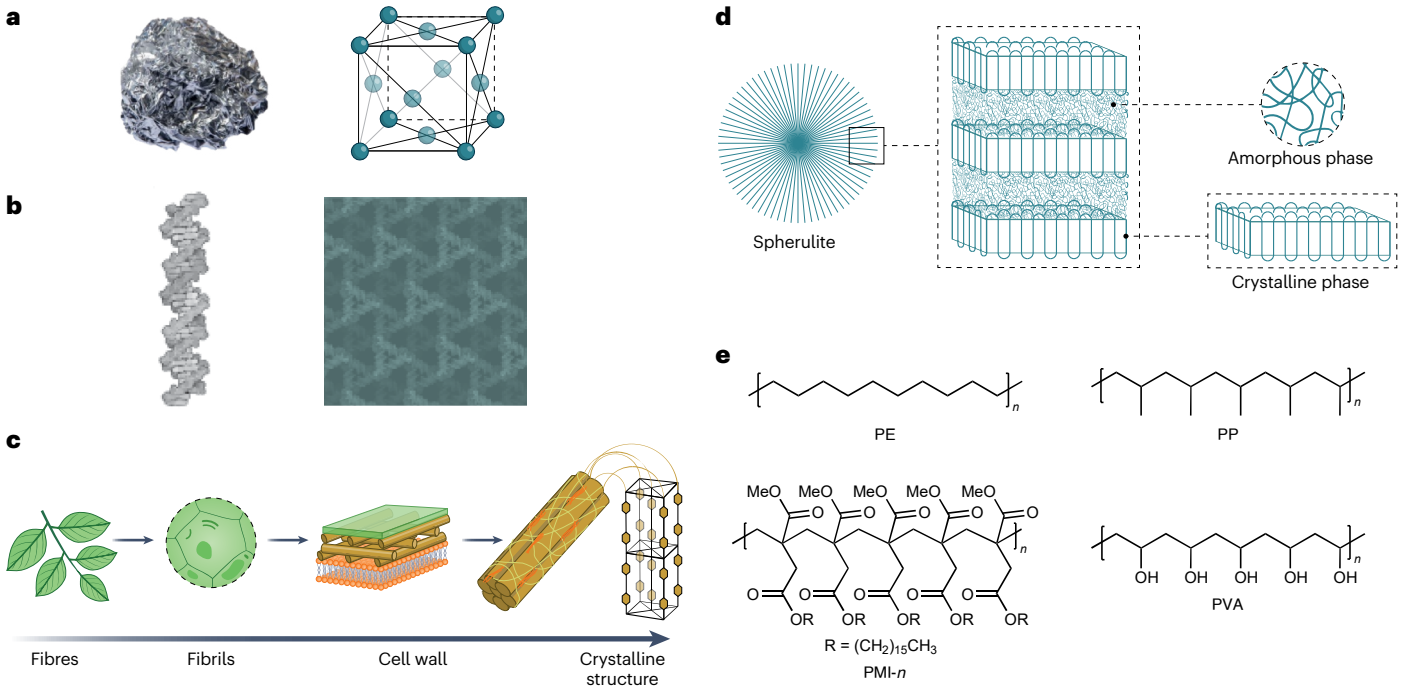


**Fig. 1 | Overview of crystalline materials in nature and in human-made materials. a**, Aluminium (left) and its crystal structure (face-centred cubic; right). **b**, Double-helix DNA structure (left) and three-dimensional lattice structure (right). **c**, Cellulose, which constitutes the fibrils that form the cell walls of plants. **d**, Spherulites, which are spherical superstructural three-dimensional entities of semicrystalline polymers composed of amorphous and crystalline phases. **e**, Examples of polymers that are able to crystallize: linear polymers such as polyethylene (PE); spatial rearrangement as in the case of polypropylene (PP); side-chain effects which are displayed in poly(mono-*n*-alkyl itaconate)s (PMI-*n*); and secondary interactions as in the case of poly(vinyl alcohol) (PVA). Credit: **a**(left), Images of Elements under a Creative Commons license CC BY 3.0; **b**, illustration sourced from PDB-101 (PDB101.rcsb.org).

that facilitates crystallization, for example, polyethylene (Fig. 1e), poly(ε-caprolactone) and poly(ethylene oxide). When the primary backbone is rigid or lacks the required regularity in its constitution and the configuration and cannot crystallize on slow cooling from the melt (for example, atactic polystyrene), crystallization can be induced by incorporating flexible regular side chains, resulting in side-chain crystallization[16–18]. In this case, side chains have a critical length to trigger crystallization, and increasing the length of the side-chain facilitates this process, as with poly(mono-*n*-alkyl itaconate)s (Fig. 1e).

A further requirement for the crystallization of polymers is the achievement of a regular conformation of minimum energy that is compatible with the chain configuration and constitution[14]. The conformation assumed by polymer chains in the crystalline state approaches one of the minima of the internal conformational energy of an isolated chain under the constraints imposed by the required symmetry that govern the crystalline state[14]. This energy minimum conformation results from intramolecular interactions that depend on the molecular structure. In the case of apolar polymers, such as polyolefins, packing effects have little influence on the conformation of the polymer chains in the crystals as long as the conformational energy of the isolated chain corresponds to a deep energy minimum[14]. Therefore, intramolecular interactions can usually dominate the final conformation of the chains within the crystal. Exceptions may be envisaged in the cases of polyisobutylene[19], poly(ethylene oxide)[19] and poly(*cis*-1,4-butadiene)[20], where the crystal field induces notable deviations from the minimum-energy conformation of isolated chains.

However, in polymers containing functional, polar groups that can provide strong intermolecular and specific interactions between different chains, such as hydrogen bonds or dipole–dipole interactions, the crystal field may strongly influence the conformation of chains in the crystals, and the adopted conformation may be different from that corresponding to the minimum conformational energy[14]. This occurs, for instance, in aliphatic polyamides, where hydrogen bonds play a key role in determining the conformation of the chains in the crystalline domains[21]. For many polymers, however, it is difficult to distinguish between intramolecular and intermolecular interactions.

An essential approach to achieving the main-chain regularity and symmetry of polymers that are needed for crystallization is to control the spatial arrangements of the bonds. For that, when the macromolecules contain stereogenic centres, they must adopt a defined configuration, and the successive configurations of consecutive stereoisomeric centres must follow specific rules. Two major stereoisomeric centres can be found in polymers: double bonds and tetrahedral centres. In the case of polymers containing double bonds, the polymers are regular when the bonds adopt all-*cis* or all-*trans* configurations. In the case of polymers with tetrahedral centres, polymers have a regular configuration if all of the centres adopt the same configuration, that is, forming an isotactic polymer, or if the centres have an alternating configuration, that is, forming a syndiotactic polymer (Box 1). In general, isotactic and syndiotactic polymers can crystallize. The absence of stereoregularity in the configurations of stereoisomeric centres results in atactic polymers that, in most cases, do not crystallize because they do not fulfil the regularity requirements of polymers for crystallization[14,22].

In the case of polymers with tetrahedral stereoisomeric centres, the degree of stereoregularity is defined by steric sequences of specific length, that is, diads, triads, tetrads or pentads, which are sequences of two, three, four or five consecutive stereoisomeric centres, respectively (Box 1). Two adjacent stereoisomeric centres that have the same configuration define a *meso* (*m*) diad, whereas if they have an opposite configuration, they define a *racemo* (*r*) diad[23–27]. Longer steric sequences, such as triads, tetrads or pentads, are composed of two, three or four consecutive *meso* or *racemo* diads, respectively. Consequently, three possible triads (that is, *mm*, *mr* and *rr*) or ten possible pentads (*mmmm*, *mmmr*, *mmrr* and so on) can be defined. The chains of an isotactic polymer comprise a regular succession of *meso* diads

## BOX 1

# Useful polymer terminology

**Semicrystalline polymer**. Polymers do not crystallize completely, unlike metals or organic compounds. The chains partially align, achieving a certain degree of crystallinity, with some chain segments constituting the crystalline phase and the other segments forming the amorphous, disordered phase.

**Tacticity**. The tacticity or stereoregularity of the polymers depends on the succession of stereoisomeric centres. In the case of polymers containing double bonds, the polymers are regular when the bonds adopt all-*cis* or all-*trans* configurations. In the case of polymers containing tetrahedral centres, polymers have a regular configuration if all of the centres adopt the same configuration, that is, an isotactic polymer, or if they have an alternating configuration, that is, a syndiotactic polymer. The absence of regularity in the conformation results in atactic polymers.

**Isotactic polymer**. Stereoregular polymer chains that consist of stereocentres with the same configuration. This type of polymer has mainly *m* diads along the chain, with the probability of *m* units being close to unity, $P_{mm} \geq 0.99$.

**Syndiotactic polymer**. Stereoregular polymer chains containing stereocentres with a perfectly alternating configuration. The chains are constituted mainly by *r* diads, with the probability of *r* units being close to unity, $P_{rr} \geq 0.99$.

**Heterotactic polymer**. Stereoregular polymers with two stereocentres having the same configuration, the next two the opposite, and so on. The chains consist only of perfectly alternating *m* and *r* diads; extending the analysis to triads, the chain displays *mr* or *rm* triads. The probability of *mr* diads is close to unity, $P_{mr} \geq 0.99$.

**Atactic polymer**. Stereoirregular polymers in which stereocentres adopt a random configuration, with the probability of *mr* diads close to 0.5, $P_{mr} = 0.5$.

**Diad**. The configuration of two adjacent stereocentres in the polymer chain. It can be *meso* (*m*) or *racemo* (*r*).

***Meso* diad**. Two adjacent stereocentres that have the same configuration, both *R* or *S*.

***Racemo* diad**. Two adjacent stereocentres that have the opposite configuration (*R* and *S*).

**Triad**. The configuration of three adjacent stereocentres. The triads can be *mm*, *rr*, *mr* or *rm* (*mr* and *rm* are usually equivalent).

**Tetrad**. The configuration of four adjacent stereocentres in the polymer chain. The tetrads can be *mmm*, *mmr*, *mrm*, *mrr*, *rmm*, *rrm*, *rmr* or *rrr*.

and, therefore, contain predominantly *mm* triads or *mmmm* pentads, and the probability of *meso* placements is close to unity, $P_{mm} \geq 0.99$ (Box 1). A syndiotactic polymer is made, instead, of a regular succession of *racemo* diads; therefore, they contain predominantly *rr* triads or *rrrr* pentads and the probability of *racemo* placements is close to unity, $P_{rr} \geq 0.99$. A heterotactic polymer comprises a regular succession of *mr* triads (…*mrmrmrmr*…) with $P_{mr} \geq 0.99$. Finally, atactic polymers are made up of a random configuration of stereocentres, with $P_{mr} = 0.5$ (refs. 23–27). The degree of stereoregularity can be evaluated, generally via NMR analysis, as the concentration of *mm* triads or *mmmm* pentads in isotactic polymers, or the concentration of *rr* triads or *rrrr* pentads in syndiotactic polymers. Other more disordered structures can also be found, such as hemi-isotactic polymers in which isospecific monomer unit placements are alternated with units of random stereochemistry. Blocky structures can also be formed, such as isotactic–atactic stereoblock polymers in which blocks of the mentioned tacticities are alternated within the polymer chain[23–27].

Whereas the preparation of stereoregular polymers is an ideal synthetic target for obtaining semicrystalline polymers, their preparation is not trivial and was not achieved until Ziegler and Natta developed Ti-based catalysts that are able to produce stereoregular polymers starting from prochiral α-olefins such as propylene[28,29]. The mechanism of the stereoselective addition of propylene via insertion into a Ti–C bond of the chiral catalyst, with the formation of chiral methine carbon centres always having the same configuration, mimics nature when stereoregular polymers such as a peptide or natural rubber are naturally produced, breaking nature's monopoly in the production of stereoregular polymers[30]. Since the discovery of stereoregular synthetic polymers, scientists have made important progress that has enabled the development of an alternative route for producing stereoregular polymers from chiral racemic monomers such as racemic lactide (D,L-lactide) using enantioselective catalysts[31]. However, the design of a catalyst that can preferentially select only one enantiomer of the racemic monomer while keeping a good reactivity/cost balance is complex from an industrial perspective. Alternatively, stereoregular polymers can also be prepared by polymerizing enantiopure, chiral monomers. However, using enantiopure monomers is necessary, and it requires several expensive and time-consuming purification and separation steps. To overcome the drawbacks of such enantioselective polymerization processes that leave the other enantiomeric monomer unreacted or require the use of enantiopure monomers that necessitate chiral separation, major strides have been made to develop more sustainable polymerization processes by developing highly stereoselective catalysts that can convert all enantiomers or diastereomers of monomers to stereoregular polymers, achieving 100% atom economy[32–36].

Some polymers, even though they are stereoirregular or atactic, can still crystallize. This phenomenon presents a considerable advantage in obtaining semicrystalline polymers as it avoids the time-consuming and expensive steps required to produce enantiopure chiral monomers or stereoselective catalysts. Some of those polymers, such as poly(vinyl alcohol) (PVA)[37] (Fig. 1e) and poly(vinyl chloride) (PVC)[38], have been known to display crystallization for decades, and it has been inferred that intermolecular interactions (such as hydrogen bonding) trigger the crystallization ability. More recently, other non-vinyl polymer families that contain main-chain C–X (X = O, S, N) bonds, such as some poly(3-hydroxyalkanoate)s (PHAs)[39] and polythioesters[40], have also been found to be able to crystallize, independent of tacticity. In these cases, the crystallization does not appear to be related to specific interactions that induce ordering. However, there is a lack of studies that investigate the origin of this ordering in such atactic polymers that lead to crystallization. Thus, atactic, yet semicrystalline, polymers are synthesized and discovered by chance and are reported as a curiosity. In this Review we summarize,

https://doi.org/10.1038/s41557-026-02113-w

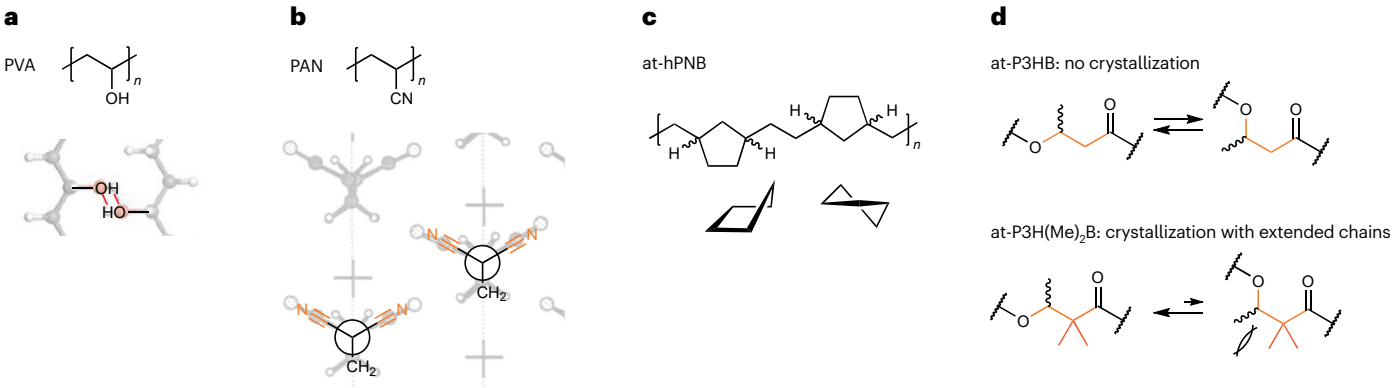


**Fig. 2 | Summary of the factors that induce crystallization in atactic polymers.** Schematic of the factors that are responsible for crystallization, displayed along with an example of a polymer including its repeating unit. **a**, Hydrogen bonds: PVA, with the hydrogen bonds highlighted in red. **b**, Dipoles: polyacrylonitrile (PAN), with nitrile groups highlighted in orange. **c**, Conformation: atactic hydrogenated polynorbornene (at-hPNB), with envelope (left) and half-chair (right) conformations of the cyclopentane ring shown. **d**, Steric effects: atactic poly(3-hydroxybutyrate) (at-P3HB) does not crystallize, but atactic poly(3-hydroxy-2,2-dimethylbutyrate) (at-P3H(Me)$_2$B), with the additional methyl groups highlighted in dark orange, does.

discuss and propose critical factors that bring specific 'order' to allow stereoirregular polymers to crystallize (Fig. 2), such as secondary interactions (for example, hydrogen bonding or electrostatic attraction (Fig. 2a,b)), conformational flexibility (Fig. 2c) or steric hindrance due to the presence of bulky groups that stabilize defective crystallizable conformations (Fig. 2d). The aim here is to provide polymer scientists with the tools to predictively design appropriate chemical structures that will lead to semicrystalline polymers despite their atactic nature.

## Requirements for atactic polymers to crystallize

### Secondary interactions

Self-assembly in nature is based on non-covalent molecular interactions. These interactions determine the material properties, and the reversibility of these interactions provides dynamism, enabling rearrangements in response to stimuli. Among non-covalent interactions, hydrogen bonds formed between an electropositive hydrogen atom and a highly electronegative atom such as oxygen, nitrogen or fluorine are among the most important and relevant to this topic. Hydrogen bonds are responsible for the self-assembly and the structure of proteins and the DNA double helix. As the hydrogen bonds are directional in proteins, to maximize the number of hydrogen bonds, the peptide bond needs to adopt a determined conformation that enables only two secondary structures: the α-helix and the β-sheet[41]. The role of hydrogen bonds in the self-assembly of complex structures expands to materials science and can promote crystallization in polymers. By incorporating functional groups that are capable of forming hydrogen bonds, such as amide or ester groups, it is possible to induce some organization between polymer chains, which can lead to semicrystalline materials[42].

**Hydrogen bonding.** An example that demonstrates the impact of hydrogen bonds in the structure of synthetic polymers can be found in PVA, where hydrogen bonds promote crystallization even when its chains are configurationally disordered[37]. PVA is obtained via the hydrolysis of poly(vinyl acetate) (PVAc) as vinyl alcohol is not stable enough (due to facile tautomerization to acetaldehyde) to perform the polymerization (Fig. 3a)[43,44]. Thus, atactic PVAc is first obtained via the radical polymerization of vinyl acetate, and then hydrolysis is performed to substitute the acetate groups in PVAc with hydroxyl groups under alkaline or acid conditions. Whereas atactic PVAc is an amorphous polymer due to a lack of stereoregularity, the resulting atactic PVA can crystallize independently of tacticity. By analysing the stereomicrostructure of the PVA via NMR, the tacticity of PVA was determined to be atactic: 21.3% isotactic (*mm*), 49.4% heterotactic (*mr*), and 29.3% syndiotactic (*rr*)[45]. Despite the atactic character, the crystal structure of PVA is characterized by chains in an ordered *trans*-planar conformation packed in a monoclinic unit cell with axes $a = 7.81$ Å, $b = 5.51$ Å, $c = 2.55$ Å and $\gamma = 92.5°$, notwithstanding the complete disorder in the succession of the configurations of the methine carbons bearing the hydroxyl group[46–48]. In fact, although the carbons of the main chain are at regular positions in the lattice, the hydroxyl groups are randomly placed in the left- and right-hand positions along the zigzag plane with the same probability. This regular conformation and packing, even in the presence of complete disorder in the positioning of the hydroxyl groups, is dictated by the establishment of hydrogen bonds between hydroxyl groups, forming sheets of chains along the 110 plane (Fig. 3a). The hydrogen bonds along the *b* axis bind these sheets together. The hydrogen bonds formed along and between the sheets force the chain to adopt a regular conformation, providing a regular structure that allows atactic PVA to crystallize[48].

PVA shows outstanding barrier properties to oxygen permeation. However, its contact with water (or moisture) should be avoided to preserve these excellent barrier characteristics. Indeed, the presence of water molecules induces plasticization of the material and slightly reduces the degree on crystallinity. The interactions of water molecules with hydroxyl groups in the polymer chain result in an increased free volume, promoting the mobility of the chains and, thus, facilitating the diffusion of water molecules through the polymer matrix for enhanced permeability[49].

The above PVA example indicates that introducing a hydroxyl group into linear polymers is a suitable strategy for facilitating their crystallization, driven by hydrogen bonding. These secondary interactions trigger the material's self-assembly, directing the arrangement between the chains and forming ordered sheets. The intermolecular hydrogen bonds between the sheets extend the order to the nano- and mesoscales.

The case of PVA indicates that the strategy of placing hydroxyl groups in a linear alkyl chain, thereby forming hydrogen bonds, may be exploited to produce various semicrystalline polymers and copolymers of differing structures. Indeed, ethylene vinyl alcohol (EVOH) copolymers have attracted much attention in the literature due to their outstanding oxygen barrier properties[50]. EVOH copolymers can be readily produced by the hydrolysis of ethylene/vinyl acetate copolymers, and they can also be synthesized via ring-opening metathesis polymerization (ROMP) and acyclic diene metathesis[51,52]. Indeed, researchers have used symmetric and achiral monomers to avoid the issues that arise from irregular insertion during propagation[52,53]. However, obtaining a polymer with a precise position of the hydroxyl group, together with

https://doi.org/10.1038/s41557-026-02113-w

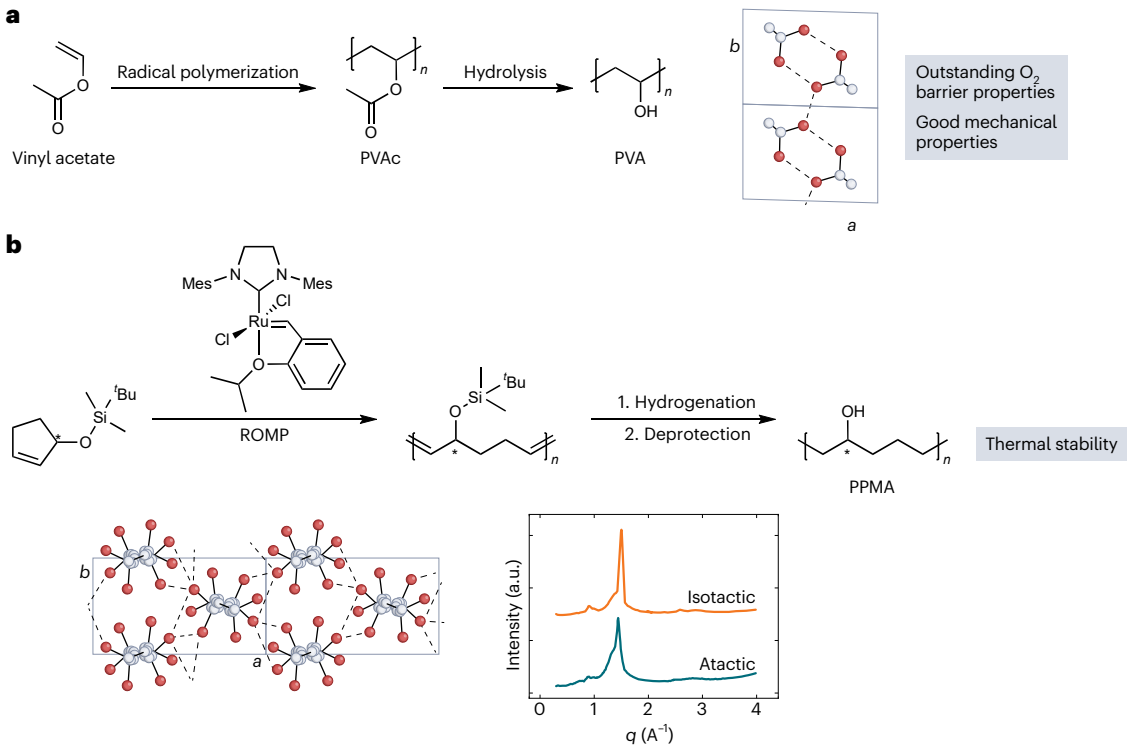


**Fig. 3 | Overview of atactic semicrystalline polymers containing hydrogen bonds. a**, Synthesis (left), crystalline structures (middle) and properties (right) of PVA, which crystallizes independently of tacticity due to the formation of hydrogen bonds between OH groups that induce the chain to adopt a regular conformation. The oxygen atoms are displayed in red, the carbon atoms are in white and the hydrogen atoms are omitted for clarity; the hydrogen bonds are indicated as dashed lines. **b**, Synthesis (top), crystalline structures (bottom left) and properties (top right) of PPMA, with the hydroxyl group placed every five carbons. The hydroxyl group promotes the alignment of the chains, obtaining semicrystalline polymers with several tacticities. Isotactic and atactic PPMA display similar WAXS patterns (bottom right). a.u., arbitrary units; Mes, mesityl.

high isotacticity, is challenging. Recently, a strategy to obtain precision polymers containing pendant hydroxyl groups to study the impact of tacticity on the crystallization of OH-group-containing polymers has been developed[54]. First, three monomers were prepared with different stereochemistry: 1*R*, 1*S* and racemic monomers. The monomers, protected with *tert*-butyldimethylchlorosilane, were subject to ROMP using the Hoveyda–Grubbs second-generation catalyst under low-temperature and close to bulk conditions. The ROMP process is highly regioregular, producing the corresponding polymer with 97% head-to-tail linkages, thus avoiding main-chain regioisomerism defects. The polymer was then deprotected, and olefin hydrogenation was performed to give the final polymer, poly(1-pentamethylene alcohol) (PPMA) (Fig. 3b)[54].

The above synthetic pathway developed to obtain PPMA makes possible the preparation of both isotactic and atactic polymers, enabling the study of their crystal structures, which is currently not possible with PVA[54]. Isotactic and atactic samples of PPMA display similar wide-angle X-ray scattering (WAXS) profiles that are characterized by the presence of one main reflection at 1.49 and 1.44 $Å^{-1}$, respectively (Fig. 3b). This proves that this polymer crystallizes independently of the tacticity, and that similar crystal structures are obtained for the isotactic and atactic polymers. Indeed, both polymers were found to crystallize in an orthorhombic unit cell with slightly longer *a* and *b* axes in the structure of atactic PPMA due to the rearrangement of chains to maximize hydrogen-bond formation in each system (Fig. 3b)[55]. In particular, the random position of the OH groups along the *trans*-planar chains of the atactic polymer enables the establishment of two types of hydrogen bond, which is achieved efficiently via a slightly bigger unit cell. In isotactic PPMA, the regular positioning of the OH groups results in only one type of hydrogen bond formed. Therefore, as in PVA, contrary to expectation, the configurational disorder with random positioning of OH groups in atactic PPMA induces a more efficient pattern of hydrogen bonds. However, the disorder reduces the melting temperature ($T_m$) from 183 °C for isotactic PPMA to 137 °C for atactic PPMA[55].

Following the above strategy, researchers have introduced a hydroxyl group on every eight carbons, showing that regioregular (head-to-tail) atactic and regio-random polymers can crystallize[56,57]. PVAc with acetate groups placed every eight carbons and highly regioregularity is also atactic and semicrystalline[58]. The mechanical, thermal and barrier properties are good, making this polymer an attractive candidate for applications such as packaging. By contrast, when the substituent groups are placed in the fourth and fifth positions, regio-irregular polymers, which are amorphous, are obtained[58]. Overall, those studies show that, to obtain semicrystalline materials, hydroxyl groups and, in some cases, regioregularity, are both required.

**Dipolar interactions.** There are other secondary interactions that induce crystallization apart from hydrogen bonds, such as dipolar interactions. Dipolar interactions play a key role in the crystallization of atactic PVC, even though the degree of crystallinity obtained is typically low. Industrially, PVC is produced mainly via the suspension radical polymerization of vinyl chloride (Fig. 4a)[59,60]. The reaction occurs through radical polymerization using appropriate initiators such as 2,2′-azobisisobutyronitrile or benzoyl peroxide. NMR studies have shown that commercial PVC obtained via radical polymerization is atactic and has the following distribution of triads: *rr* 29.1%, *mm* 18.8% and *mr* 52.0%. The polymerization method and reaction temperature impact the percentage of syndiotactic triads and the degree of crystallinity. Decreasing the polymerization temperature increases the

https://doi.org/10.1038/s41557-026-02113-w

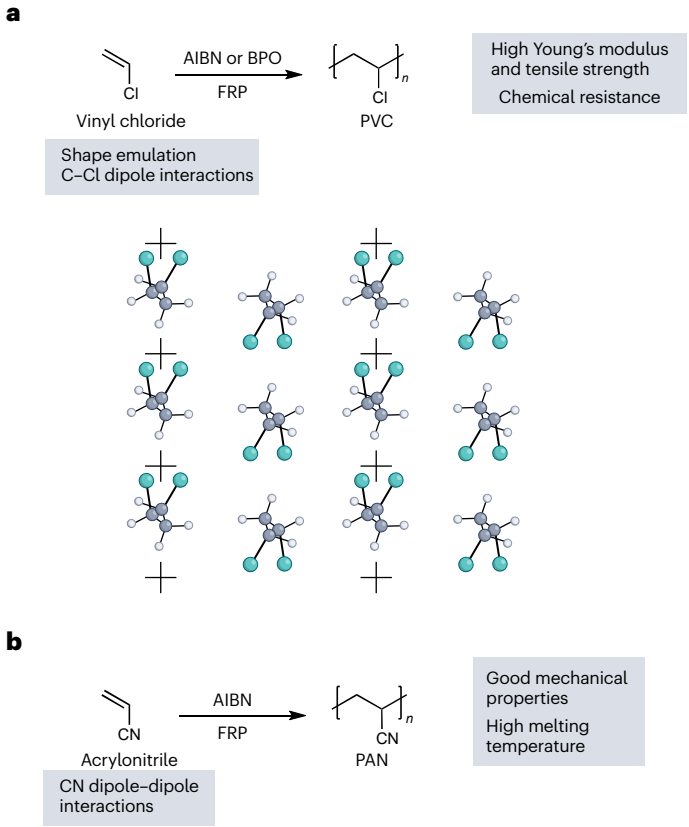


**Fig. 4 | Overview of atactic semicrystalline polymers containing dipolar interactions. a**,**b**, Synthesis of PVC (**a**) and PAN (**b**) via free-radical polymerization (FRP). Dipole interactions between C–Cl groups and CN groups are responsible for the conformations of the chains in the crystal. Some of the relevant physical properties are mentioned for each polymer (right), with both displaying good mechanical performance. The representative *c*-axis projection of PVC crystalline structure (based on ref. 62). AIBN, 2,2′-azobisisobutyronitrile; BPO, benzoyl peroxide.

amount of syndiotactic triads and enhances the crystallinity[61]. The chains of the atactic PVC generated via free-radical polymerization are characterized by the presence of relatively short syndiotactic (*rr*) sequences, alternating with irregular and even short isotactic (*mm*) sequences. Initially, it was thought that the crystallization of atactic PVC was due to the crystallization of the syndiotactic sequences that assume a regular *trans*-planar conformation and pack in an orthorhombic unit cell[61–64]. However, the non-negligible degree of crystallinity (about 10%) cannot be explained by the crystallization of the solely short syndiotactic sequences, as the crystallizable sequences are longer than the syndiotactic ones and should also include the irregular or short isotactic chain segments. Therefore, the isotactic sequences are incorporated in the crystals together with the syndiotactic segments because the isotactic segment can adopt a specific conformation that is similar in shape to the *trans*-planar conformation of the syndiotactic segments, providing an example of crystallization driven by shape emulation (Fig. 4a)[62]. Moreover, C–Cl dipole interactions further stabilize this conformation, which finally induces crystallization. Notably, PVC displays good mechanical properties (although it is brittle), high chemical resistance and high transparency. The mechanical performance can be tuned with the addition of plasticizers, which results in PVC-based materials with a variety of properties from rigid to flexible materials[65].

Polyacrylonitrile (PAN) is a special case of an atactic polymer where intramolecular dipole interactions between nitrile groups drive the chain conformation and induce conformational disorder that does not prevent crystallization, notwithstanding the configurational disorder and consequent conformational disorder. The crystallinity of PAN fibres drawn from atactic PAN has been widely investigated, as they serve as precursors to carbon fibres. PAN is obtained from the radical polymerization of acrylonitrile (Fig. 4b)[66–68], and industrially, PAN is synthesized through the aqueous emulsion polymerization of acrylonitrile. With this free-radical polymerization process, the PAN obtained has very little stereoregularity, with triad concentrations of 49% *mr*, 23% *rr*, and 28% *mm*. This triad distribution is very close to that expected for the Bernoulli-type statistics of a completely atactic polymer with equal *m* and *r* diad concentrations and 2:1:1 ratio of heter otactic:syndiotactic:isotactic triads[69,70]. The stereoirregular chains can crystallize, and crystals of PAN are characterized by long-range order only for the position of chain axes arranged on a pseudohexagonal lattice with $a = b = 6$ Å (refs. 71–73). The conformation of the stereoirregular chains is also disordered, but the disorder maintains a long-range positional order of the chain axes on the hexagonal lattice. The chain periodicity of nearly 2.4–2.5 Å indicates that the pseudohexagonal crystalline form of PAN is formed by the crystallization of elongated portions of chains with a prevailing syndiotactic configuration in a nearly *trans*-planar conformation. However, the hypothesis that only syndiotactic sequences in a fully planar conformation will crystallize is inconsistent with the distribution of stereosequences and the low value of the chain axis. This indicates that the crystallizable sequences include *meso* sequences and conformational disorder that shortens the mean repetition period to 2.4 Å per monomeric unit, consistent with the high value of the crystalline density. In ref. 73 it was suggested that the chain conformation close to *racemo* diads is nearly *trans*, with deviations of 10° from 180° in the torsion angles that alleviate repulsive electric forces between nitrile groups, whereas the backbone bonds close to *meso* diads may deviate largely from 180°, and some bonds may assume torsion angle close to a *gauche* conformation; these distortions shorten the mean repetition period from $c = 2.5$ Å for a perfect *trans* conformation to 2.3–2.4 Å per monomeric unit and alleviate unfavourable electrostatic interactions between adjacent CN groups[14,74]. In this irregular conformation, the presence of *gauche* bonds in crystallizable portions of atactic chains will rotate the mean plane of the backbone chain by nearly 120°, with the result that –CN side groups project perpendicularly to the chain axis along directions placed at ~120° to each other[73], minimizing the steric hindrance and the intramolecular electrostatic repulsive interactions between CN groups.

Solid-state NMR studies performed on PAN samples with chains labelled with $^{2}H$ and/or $^{13}C$ at suitable positions, to selectively enhance the NMR signals of atoms in *meso* and *racemo* diads, have enabled a direct and detailed analysis of the local structure and of the conformational disorder of PAN in the solid state[75–77]. The results indicate that, in this disordered conformation, the *trans*:*gauche* ratio is close to 90:10, and most of the *meso* diads assume a largely distorted *trans* conformation. Moreover, the torsion angles in the *trans* states of *meso* diads and *racemo* diads are largely different because of the steric hindrance and electronic dipole repulsive force of –CN groups in the *meso* diad[76]. From this NMR analysis, it was found that the torsion angles of the bonds inside *meso* sequences in the *trans* state deviate notably from the ideal *trans* conformation by 10–20°. In the *racemo* diad, the *trans* state instead assumes the ideal *trans* conformation (180°)[77]. This specific conformation identifies conformational disorder where the high *trans* content is enabled by the torsion angle deviations from the ideal *trans* state in *meso* diads in the *trans* state, which alleviates the steric hindrance and the large intramolecular repulsive electric dipole interactions between the CN groups in the *mm* configuration and thus lowers the intramolecular conformational energy[76]. Semiquantitative information on intermolecular alignment was also obtained from detailed analyses of two-dimensional NMR spectra[77], indicating that the –CN side groups are mostly oriented along the crystalline lattice

directions $a$, $b$ and $-(a+b)$ of the hexagonal lattice, similar to what was indicated in the structural model proposed in refs. 73,74.

The structure of PAN with the described conformational disorder is, therefore, a result of both intra- and intermolecular interactions. Notably important in PAN are the intramolecular electric repulsion force and steric hindrance[76]. The structure also accounts for its excellent mechanical properties. PAN exhibits a high glass transition temperature, $T_g$, (above 100 °C) and a high modulus that reaches 28 GPa (refs. 78–80). Indeed, contrary to expectation, the excellent mechanical properties arise from the disordered configuration and the disorder in the chain conformation rather than from intermolecular dipole interactions due to the presence of polar CN groups. The molecular dynamics in stereoirregular polymers play an important role[81]. Specifically, the configurational disorder coupled with conformational flexibility may lead to fast chain dynamics in the crystalline phase[81]. In the structure of PAN, the atactic configuration and the conformational disorder[75] contribute to the molecular dynamics of crystalline chains due to additional space in the atactic configuration. Such molecular dynamics facilitate chain slippage and molecular orientation during processing, resulting in an excellent fibre material.

In summary, atactic vinyl polymers containing polar functional groups, such as OH, Cl and CN, as highlighted above, can crystallize due to the secondary (hydrogen bonding or dipolar) intra- and intermolecular interactions induced by these functional groups. The requisites for this crystallization behaviour are the flexibility of the chain backbone and the regularity of the repeating unit structure to some extent. With that, the energetically favoured conformation is *trans*-planar or nearly *trans*-planar, allowing the packing of atactic chains that have a random stereoconfiguration of chiral backbone carbons and a random conformation of substituent groups.

### Conformational flexibility

Some cyclic alkane molecules, such as cyclopentane or cyclohexane, have conformational flexibility arising from C–C bond rotation in the crystalline state[81]. The crystalline materials formed from such cyclic alkanes are known as plastic crystals as they show order in the position of the barycentre of the molecules, similar to a crystal, but have local mobility and corresponding disorder in the orientation of the molecules[82]. There are several examples of plastic crystals, such as camphor, found in the wood of the *Cinnamomum camphora* tree, or adamantane, used in drugs or lubricants. Spherical molecules usually form those plastic crystals, which can create a plastic crystal phase with isotropic rotator motion, so there is a random molecular orientation. Still, the molecular centre of gravity is kept in the crystal lattice, displaying three-dimensional long-range order[83]. These plastic crystals are mechanically deformable due to the migration of defects instead of being as rigid and brittle as conventional crystals.

Cyclopentane and cyclohexane adopt non-planar puckered conformations with the hydrogen atoms positioned above and below the plane[84]. The flat potential energy surface of cyclopentane allows the ring to pseudorotate between the half-chair and envelope conformations[85–87]. Owing to the rotation of C–C bonds, incorporating such units into a polymer backbone can induce conformational flexibility. Intra- and intermolecular interactions contribute to determine the conformation and packing, which includes conformational flexibility. All of these effects lead to the crystallization of polymers, even when they are atactic. This is the case for hydrogenated polynorbornene (hPNB) materials, in which isotactic, syndiotactic and atactic hPNB can all crystallize[81].

The production of hPNB is via the ROMP of norbornene, followed by hydrogenation of the double bonds in the resulting PNB (Fig. 5a). Several catalysts have been used to synthesize hPNBs with different tacticities. Syndiotactic hPNB, with an *m*:*r* ratio of 10/90, was synthesized using $WNPhCl_4Et_2O$ as the catalyst[88] Isotactic hPNB, with an *m*:*r* ratio of 100/0, was synthesized using MoO(*rac*-biphenolate)$_2$ as the catalyst. Atactic hPNB was synthesized using the Grubbs second-generation catalyst (G2), with an *m*:*r* ratio of 53/47 (Fig. 5a)[88].

The structure of hPNB consists of alternating cyclopentane rings and ethylene units along the chain, with various stereoregularities[89–91]. As a saturated hydrocarbon polymer, hPNB exhibits only dispersive interactions between the chains, and the stereoirregularity arises from the cyclopentane rings. The even number of methylene units in hPNB causes the cyclopentane rings to adopt opposite orientations when the backbone is extended into the *trans* zigzag conformation. X-ray studies have shown that hPNBs have a repeating period along the chain axis close to 12.5 Å. Hence, across all three hPNB samples with various tacticities, the skeletal chains adopt a similar *trans*-planar zigzag conformation with slight torsional angle fluctuations around the skeletal C–C bonds, with the cyclopentane rings integrated as the parts of the skeletal chains (Fig. 5a)[88]. However, the $CH_2$–$CH_2$ side groups of the rings protrude from the skeletal chain in different orientations, depending on the tacticity, resulting in remarkable variations in the overall chain shape and, consequently, the chain-packing structure. As is shown in their WAXS profiles, the crystalline structure depends on the tacticity (Fig. 5a). Syndiotactic hPNB adopts a monoclinic unit cell with dimensions $a = 5.97$ Å, $b = 9.48$ Å, $c = 12.58$ Å and $\beta = 60.0°$. The cyclopentane rings are placed along the chain axis with two $CH_2$ units out of the plane. Isotactic hPNB crystallizes in an orthorhombic unit cell with dimensions $a = 5.95$ Å, $b = 8.25$ Å and $c = 12.65$ Å. The conformation of the main chain is the same as for the syndiotactic polymer, with the two cyclopentane rings alternatingly located on the right- and left-hand sides of the chain. Atactic hPNB crystallizes in an orthorhombic unit cell with dimensions $a = 5.43$ Å, $b = 9.45$ Å and $c = 12.41$ Å, slightly larger than the isotactic polymer. Atactic chains adopt a *trans*-planar conformation with the rings located on the right- and left-hand sides of the planar zigzag chain with 50% probability. Therefore, the configurational disorder on the main-chain stereocentres in atactic hPNB is such that the nearly *trans*-planar conformation is maintained, allowing crystallization despite the statistical positioning of the ring along the chains, and a lateral packing of the chains similar to that of isotactic hPNB is achieved.

According to the crystal structures, isotactic, syndiotactic and atactic hPNBs display similar melting temperatures, with $T_m = 178$ and 145 °C for the isotactic and atactic hPNBs, respectively, which are higher than that for syndiotactic hPNB ($T_m = 134$ °C)[92]. Moreover, the isotactic and atactic hPNBs show additional endothermic transitions in the differential scanning calorimetry heating curves at temperatures slightly lower than the corresponding melting temperatures (150 and 120 °C, respectively). These transitions have been attributed to the activation of further disorder in the structures due to conformational changes in the isotactic polymer, with some C–C bonds transforming from the *trans* to the *gauche* conformation that results in a high-temperature orthorhombic phase with larger $a$ and $b$ dimensions and a shorter $c$ axis, and rotational motion of the ring side groups in the atactic polymer that retains a nearly *trans* conformation and exhibits fast chain dynamics, driven by amplified C–C bond rotations. Both transitions lead to increased structural disorder in the crystal structure of the isotactic and atactic polymers before melting, with a corresponding decrease in the melting entropy, explaining the higher melting temperatures, particularly for the atactic polymer, compared with that of the syndiotactic polymer[81]. The combination of configurational disorder coupled with the conformational flexibility of atactic hPNB results in a crystal–crystal transition, fast dynamics around the chain axis and structural evolution[81].

The selectivity of the hydrogenation process affects the structure, varying the amount of *cis* and *trans* cyclopentane rings and, thus, the crystallinity. A study was carried out using solely the *cis* configuration with an *m*:*r* ratio of 1.1 (ref. 89). The stability of the rotationally ordered polymorph decreases with higher levels of epimerization, as indicated by a reduction in the cold crystallization temperature, $T_{cc}$, from 134 °C

https://doi.org/10.1038/s41557-026-02113-w

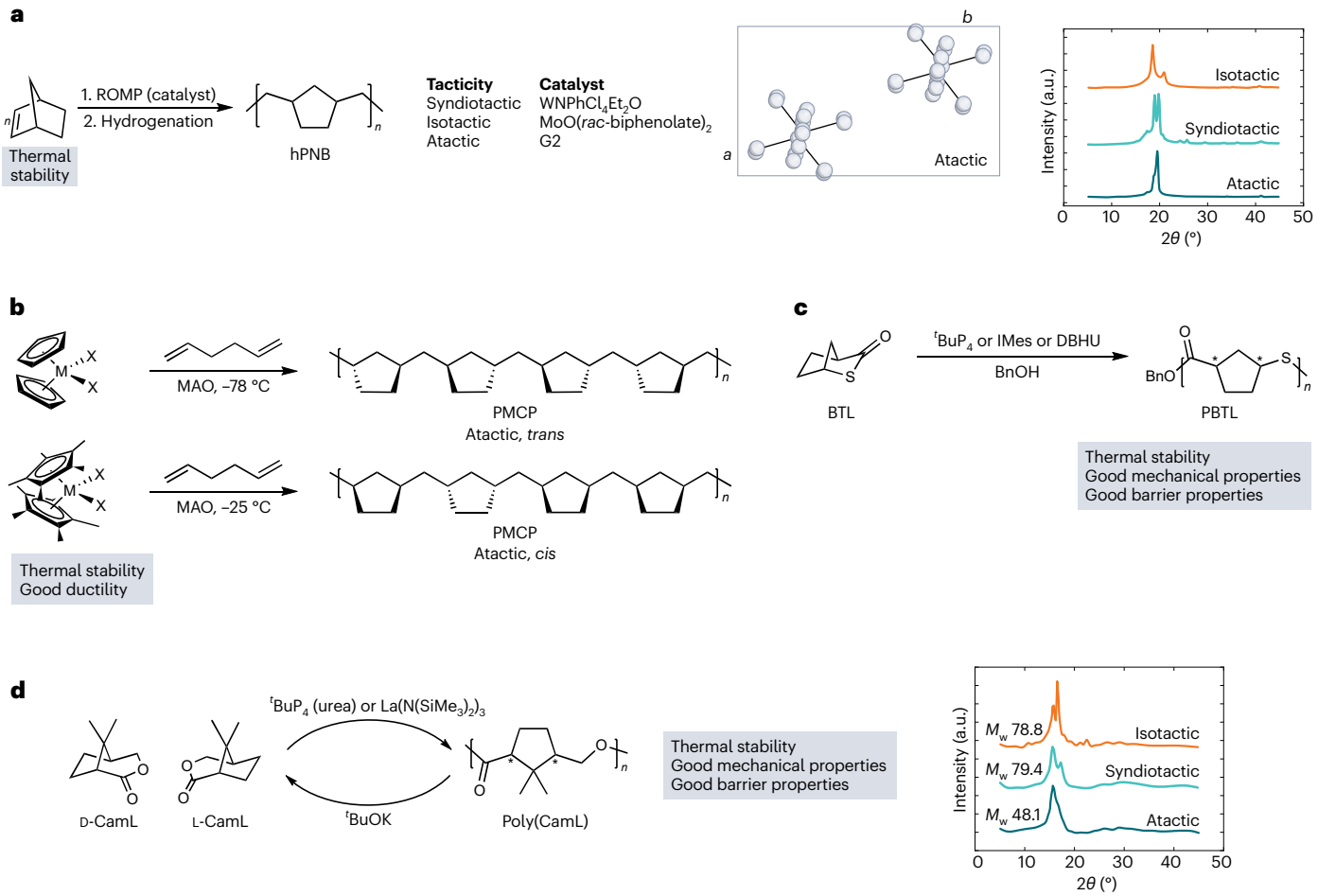


**Fig. 5 | Overview of semicrystalline polymers with conformational flexibility.** **a**, Synthesis, properties and crystalline structure of hPNBs. The catalysts used for synthesizing hPNB with different tacticities are shown. The crystalline structure of atactic hPNB is shown alongside the WAXS patterns of isotactic, syndiotactic and atactic hPNB. $2\theta$, scattering angle. **b**, Reaction conditions for the synthesis of atactic, *trans*-PMCP and atactic, *cis*-PMCP, with the characteristic physical properties shown. MAO, methylaluminoxane. **c**, Reaction conditions for the synthesis of PBTL, and its properties. $^{t}BuP_4$, 1-*tert*-butyl-4,4,4-tris(dimethylamino)-2,2-bis[tris(dimethylamino)phosphoranylidenamino]-2λ$^5$,4λ$^5$-catenadi(phosphazene); IMes, 1,3-bis(2,4,6-trimethylphenyl)imidazol-2-ylidene; DBU, 1,8-diazabicyclo[5.4.0]undec-7-ene; BnOH, benzyl alcohol; *, chiral centre. **d**, Polymerization and depolymerization conditions for poly(CamL), including the WAXS patterns of the atactic and isotactic polymers and their physical properties. CamL, camphor-derived lactone; $M_w$, weight-averaged molecular mass.

with 0% epimerization (with diimide) to 122 °C with 1.7% epimerization (with Ni/Al complex) and 92 °C with 22% epimerization (with Pd(0))[89,91].

The same strategy of introducing a cyclopentane group that brings conformational flexibility has been used in poly(methylene-1,3-cyclopentane) (PMCP), obtaining an atactic semicrystalline polymer (Fig. 5b)[93]. It contains only one methylene group between two adjacent cyclopentane rings in the main-chain backbone. This polymer forms similar, highly disordered crystal structures regardless of the microstructure and tacticity. The crystalline phase of all stereoregular and irregular samples consists of parallel extended chains packed in a pseudohexagonal lattice with configurational and conformational disorder, which generates nearly complete intermolecular rotational and translational disorder along the chain axes[85,93–101].

Systematic studies have been extended to hydrocarbon polymers with varying numbers of $CH_2$ groups (for example, 1, 3, 4 or 10) between 1,3-disubstituted cyclopentane structures. These polymers were synthesized through isomerization polymerization of 4-alkylcyclopentenes, catalysed by Pd complexes via an olefin insertion and chain walking mechanism[102]. All four atactic hydrocarbon polymers are semicrystalline with $T_m$ values ranging from 60 to 86 °C, highlighting the crucial role of cyclopentane units in overcoming configuration disorder. The substitution site of the cyclopentane units also influences the crystallization behaviour[103]. Indeed, in polyethylene containing random arrays of varying amounts of *cis*- and *trans*-1,3-cyclopentylene units, the rings are incorporated into the polyethylene crystal structure. However, in the case of 1,2-disubstituted cyclopentane structures, the rings are excluded from the crystalline phase and remain in the amorphous phase.

Ester groups can be incorporated into these kinds of polymers, leading to polyesters with cyclohexane or cyclopentane rings in the main backbone. Poly(cyclohexene dihydrocoumarate) and poly(cyclopentene dihydrocoumarate) were synthesized by alternating ring-opening copolymerization of dihydrocoumarin with cyclohexene epoxide or cyclopentene epoxide, catalysed by chromium(III) salen complexes[104]. Those polymers exhibited a high degree of crystallinity, with $T_m$ values of 139 °C and 173 °C, respectively. Cyclopentane and cyclohexane rings, with their non-planar (puckered) ring structures, provide additional conformational flexibility through C–C bond rotation in the solid state. Despite this flexibility, these two tacticity-independent crystalline polyesters require several hours of annealing to crystallize, indicating slow crystallization kinetics.

The strategy of incorporating functional groups in polymers containing cyclohexane or cyclopentane rings in the main backbone has been extended to polythioesters. Hence, recently, a few

https://doi.org/10.1038/s41557-026-02113-w

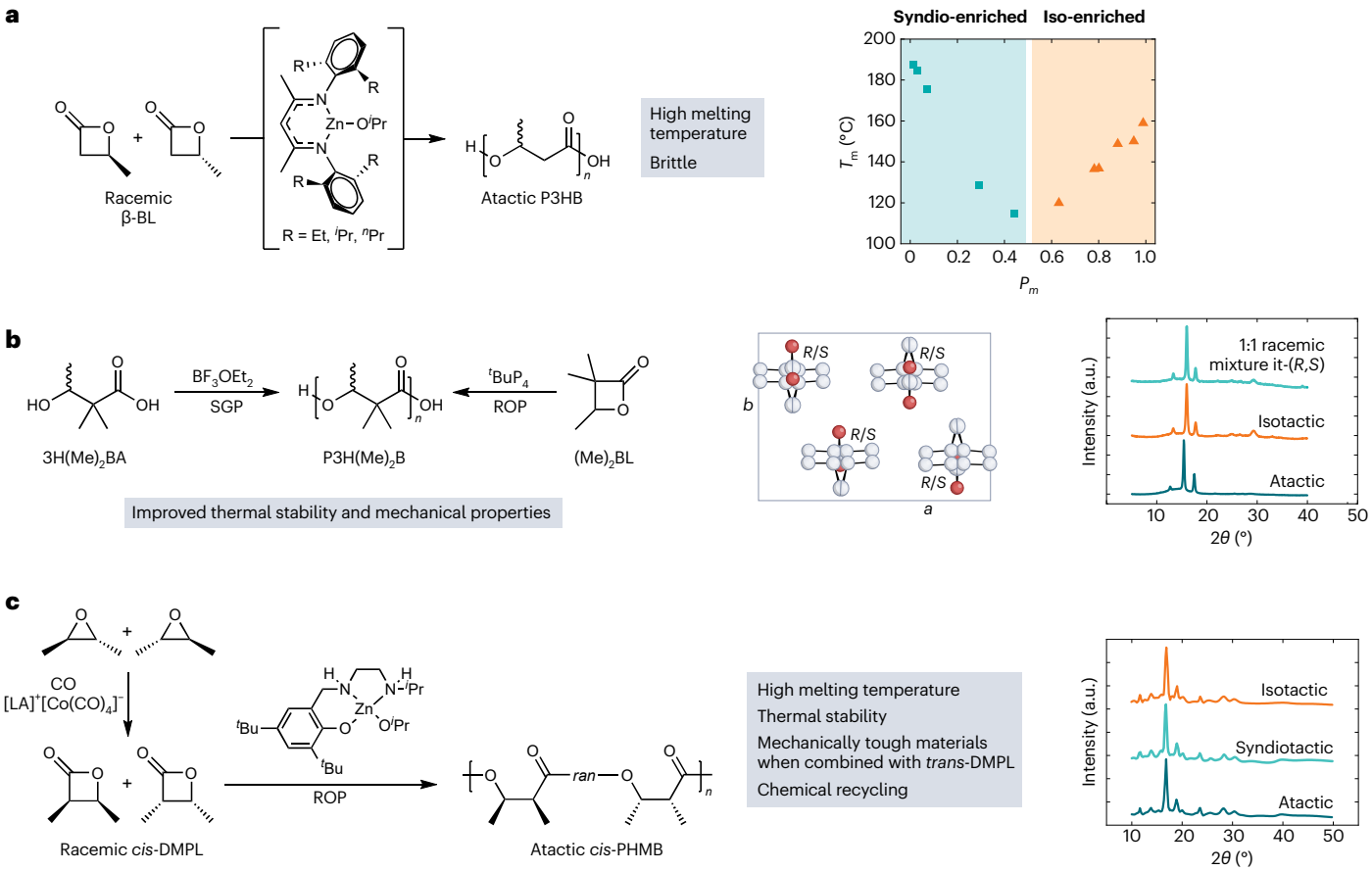


**Fig. 6 | Overview of atactic semicrystalline polymers with steric effects.** **a**–**c**, Synthesis, properties and crystalline structures of atactic P3HB, which is amorphous (**a**), P3H(Me)$_2$B (**b**) and PHMB (**c**). In **a**, the plot displays the melting temperature as a function of tacticity. For $P_m = 0.5$, which corresponds to the atactic sample, there is no $T_m$ as the sample remains amorphous. BL, butyrolactone. In **b**, P3H(Me)$_2$B can be synthesized via the step-growth polymerization (SGP) of the hydroxyacid or via ring-opening polymerization (ROP) of the lactone. Crystalline unit cell of the atactic sample and WAXS patterns of the atactic, isotactic and racemic mixture, where it-(*R*,*S*) denotes isotactic (*R*,*S*)-P3H(Me)$_2$B. 3H(Me)$_2$BA, 3-hydroxy-2,2-dimethylbutyric acid. In **c**, the full synthesis of PHMB is shown, including the synthesis of the monomer and the corresponding ring-opening polymerization. WAXS patterns of the isotactic, syndiotactic and atactic polymers. LA, Lewis acid; *ran*, random.

chemically recyclable polythioesters that crystallize independently of tacticity have been reported. For example, poly(2-thiabicyclo[2.2.1]heptan-3-one) (PBTL) with linear or cyclic topology[40] exhibits tacticity-independent crystallinity (Fig. 5c) and rapid crystallization kinetics, with a tunable $T_m$ ranging from 166 to 213 °C as the probability of forming a *racemo* diad during polymer chain growth ($P_r$) varies from 0.24 to 1.00. The atactic polymer ($P_r = 0.47$) displays a $T_m$ of 184.0 °C. The configurational disorder, coupled with the conformational flexibility introduced by the cyclopentane units in PBTL, provides additional chain dynamics, contributing to its unique crystallinity, similar to other cyclopentane-containing polymers. The highest $T_m$ of 213 °C was observed in perfectly syndiotactic PBTL, regardless of whether it had a cyclic or linear topology. Typically, the high degree of crystallinity is associated with an increased tensile strength but also with brittleness—a well-known trade-off in semicrystalline polymers. However, in the case of atactic PBTL, its tacticity-independent crystallinity imparts high strength and stiffness, with an ultimate tensile strength of 41.4 MPa and a Young's modulus of 2.0 GPa. At the same time, the inherent single-chain-level disorder preserves its ductility, achieving an appreciable elongation at break of over 200%. By contrast, the perfectly syndiotactic PBTL is a brittle material.

A polyester analogue to PBTL, poly(2-oxabicyclo[2.2.1]heptan-3-one) (PBL), exhibits a $T_g$ of 18 °C, which is lower than that of atactic PBTL (58 °C) and perfectly stereo-ordered PBTL (118 °C). The as-prepared atactic PBL was a transparent and soft elastomer, but after being left at room temperature for one month, it turned into an opaque and hard plastic with a $T_m$ of 54 °C. The $T_m$ of syndio-enriched PBL ($P_r = 0.97$) is 144 °C. These results indicate that the 1,3-disubstituted cyclopentane units in PBL, with their conformational flexibility, can also tolerate configurational disorder and facilitate chain packing and crystallization. However, replacing the thioester bond with an ester bond reduces notably the crystallization kinetics. Notably, 1,3-disubstituted cyclohexane units do not seem to facilitate the well-defined chain packing necessary for crystallization. For instance, atactic poly(6-oxabicyclo[3.2.1]octan-7-one) (PBiL) did not exhibit crystallinity[105]. The $T_g$ of PBiL is 130 °C, compared with the $T_g$ of 18 °C for PBL, indicating that simply leaving PBL at room temperature (~25 °C) can be considered an annealing process, whereas, for PBiL, annealing would need to occur above its $T_g$ (130 °C).

Notably, poly(CamL)[106], a similar polyester but with an additional methyl group in the main backbone and a *gem*-dimethyl-substituted cyclopentane group, displays tacticity-independent crystallization (Fig. 5d). WAXS profiles display different main reflections depending on the tacticity, which may indicate a different chain packing (Fig. 5d). The presence of the dimethyl groups on the 1,3-disubstituted cyclopentane unit may account for its relatively fast crystallization kinetics compared with PBL. Further exploration is warranted to gain deeper insights into whether 1,3-disubstituted cyclohexane units can overcome configurational disorder through conformational flexibility in the polyester systems.

In summary, incorporating cyclopentane or cyclohexane rings in the polymer backbone induces conformational flexibility, allowing C–C rotation. Despite the configurational disorder, the stereoirregular chains can pack, due to the conformational flexibility brought about by the cycloalkane rings, adopting typically a *trans*-planar conformation. The structure of the chains can be modified by incorporating different functional groups in the main backbone or the number of methylene groups without losing the ability to crystallize.

### Steric effect inducing defective crystallizable conformation

In most polymers, the conformation of the chains in the crystalline state is defined by non-bonding interactions between the atoms. In particular, in apolar poly(α-olefin)s, the van der Waals interactions between neighbouring atoms of the side groups induce iso-distortions of the torsion angles from the minimum-energy *trans* conformation towards the *gauche* conformation and stabilization of helical conformations with *M*/*N* symmetry (that is, the 3/1 helical conformation of isotactic polypropylene (PP) compared with the *trans*-planar conformation of polyethylene)[14,25]. An intriguing, similar effect but with the opposite outcome has recently been found in some PHAs[109], which have gained considerable attention in the past decades as they can be obtained from renewable sources via both biological and chemical routes. In addition, they can be biodegraded or chemically recycled once they reach their end of life.

Among the PHAs, poly(3-hydroxybutyrate) (P3HB) has been the most produced and investigated. Isotactic P3HB and syndiotactic P3HB are crystalline, whereas atactic P3HB does not crystallize and is an amorphous polymer. Indeed, P3HB samples with various values of the probability of forming a *meso* diad during polymer chain growth ($P_m$) have been synthesized, covering a wide range of $P_m$ going from highly isotactic ($P_m$ close to unity) to highly syndiotactic ($P_m$ close to zero). The study shows that P3HB can crystallize over the entire range except at $P_m$ values close to 0.5 (Fig. 6a). P3HB samples with $P_m$ values of 0.45 or 0.63 crystallize; however, P3HB with a $P_m$ value of 0.45–0.55, close to the atactic one ($P_m$ = 0.5), remains amorphous[107]. Getting further away from perfectly isotactic ($P_m$ = 1) or syndiotactic ($P_m$ = 0) polymers, $T_m$ decreases due to the increase in entropy on the basis of $T_m° = \Delta H/\Delta S$, where $T_m°$ is the equilibrium melting temperature, $\Delta H$ is the melting enthalpy and $\Delta S$ is the melting entropy. Isotactic P3HB crystallizes in the most stable α-form, with chains in 2/1 helical conformation packed in an orthorhombic unit cell with axes $a$ = 5.73 Å, $b$ = 13.15 Å and $c$ = 5.93 Å. With tensile deformation, the α-form transforms into the less stable β-form, which is characterized by chains in the *trans*-planar conformation packed in a hexagonal unit cell with dimensions $a = b$ = 9.22 Å, $c$ = 4.66 Å and $\gamma$ = 120° (ref. 108).

Substituting the two hydrogen atoms on the α-carbon atom of P3HB with two methyl groups gives poly(3-hydroxy-2,2-dimethylbutyrate) (P3H(Me)$_2$B), which shows improved thermal stability and intrinsic crystallizability, that is, the polymer can crystallize independently of tacticity. P3H(Me)$_2$B has been synthesized via two strategies (Fig. 6b)[39]. One is via the step-growth polymerization of the hydroxyacid 3H(Me)$_2$BA with $BF_3OEt_2$ as the catalyst. This AB-type hydroxyacid monomer was synthesized in one step, using isobutyric acid and acetaldehyde. The second strategy is the ring-opening polymerization method. First, lactonization of the hydroxyacid was conducted on the lactone monomer. Afterwards, ring-opening polymerization of the cyclic lactone was carried out using the organic superbase catalyst $^t$BuP$_4$.

The isotactic and atactic P3H(Me)$_2$B materials show identical X-ray diffraction profiles (Fig. 6b), indicating that they crystallize in the same crystal structure[109]. The ordered chiral isotactic P3H(Me)$_2$B crystallizes with chains in a distorted *trans*-planar conformation in an orthorhombic unit cell with axes $a$ = 13.30 Å, $b$ = 9.99 Å and $c$ = 4.75 Å according to the chiral space group $P2_12_12$, contrary to P3HB that crystallizes with chains in the two-fold helical conformation (Fig. 6). Atactic P3H(Me)$_2$B assumes a similar distorted *trans*-planar conformation that keeps the chains straight and with the same periodicity as the isotactic polymer, despite the complete configuration disorder. This disordered conformation of the atactic chain assumes nearly the same shape as the isotactic chains, explaining why the atactic polymer can crystallize and providing an example of crystallization driven by shape emulation. The atactic chains in the disordered conformation can pack in the same orthorhombic unit cell as the isotactic polymers with only slightly larger dimensions, $a$ = 13.94 Å, $b$ = 10.03 Å and $c$ = 4.75 Å. Therefore, this configuration disorder and the corresponding conformational disorder do not prevent packing in the same unit cell as the isotactic polymer. This represents an example of the crystallization of atactic and isotactic polymers in the same crystal structure.

The crystallization of P3H(Me)$_2$B, in which a distorted *trans*-planar conformation is adopted in both the isotactic and atactic polymers, is in contrast to P3HB, which assumes a 2/1 helical conformation in the stable α-form—this is a straightforward consequence of replacing the two α-hydrogen atoms in P3HB with two methyl groups[109]. Whereas in P3HB the 2/1 helical conformation is the most stable conformation, the steric interactions arising from the presence of the two methyl groups in P3H(Me)$_2$B make the *trans*-planar and the 2/1 helical conformations nearly isoenergetic. However, both isotactic and atactic P3H(Me)$_2$B do not show polymorphism, and only the chains in the *trans*-planar conformation crystallize, presumably due to more efficient packing. Therefore, in this PHA, the steric interactions due to the presence of bulky side groups stabilize the *trans*-planar conformation compared to the helical conformation, which is the opposite outcome to what occurs in polyolefins. The assumed *trans*-planar conformation, in turn, minimizes the effect of configurational defects in atactic P3H(Me)$_2$B, whose chains assume a similar distorted *trans*-planar conformation and have the same shape as that of the isotactic chain and, hence, can pack in the same unit cell. This explains the crystallization of atactic P3H(Me)$_2$B in the same crystal structure of the isotactic polymer with the only difference being that, due to the higher degree of disorder, the atactic polymer melts at a lower temperature (176 °C) than that of the isotactic polymer (243 °C). This tacticity-independent crystallization, finally, results in the much superior mechanical properties of atactic P3H(Me)$_2$B over the parent P3HB, with remarkably improved ductility.

The two α-protons in the parent P3HB are responsible for thermal degradation following a *cis* elimination process. By substituting those two protons with methyl groups in P3H(Me)$_2$B, the thermal stability of this PHA is notably improved, enabling the processing of this material in the melt state. The inclusion of the methyl groups also resulted in improved mechanical properties, with ductile behaviour ($\varepsilon_b$ = 228%), high elastic modulus ($E$ = 2.92 GPa) and high ultimate stress ($\sigma_b$ = 31.6 MPa) values that are comparable to certain grades of commercial isotactic PP and high-density polyethylene. The mechanical extensibility is much better than that of isotactic P3HB, which is extremely brittle ($\varepsilon_b$ = 3–6%). In addition, P3H(Me)$_2$B is chemically recyclable as it can be depolymerized back to the original monomer, closing the chemical loop[39]. Thus, with this α,α-disubstitution strategy, thermal degradation, brittleness and inability to depolymerize back to the four-membered lactone monomer are overcome for P3HB, providing a mechanically robust, melt-processable and chemically recyclable PHA.

Similar crystallization behaviour has been found in monomethylated P3HB, where only one α-hydrogen atom is replaced with a methyl group, resulting in the presence of two chiral centres (Fig. 6c)[110]. Moreover, in this case, isotactic, syndiotactic and atactic poly(3-hydroxy-2-methylbutyrate) (PHMB) materials show similar X-ray diffraction profiles (Fig. 6c), indicating crystallization in a similar crystal structure, although the crystal structure was not reported. To synthesize PHMB, first, 2,3-dimethyl-β-propiolactone (DMPL) was synthesized by the catalytic carbonylation of 2-butene oxide with CO, *meso*-tetraphenylphorphyrinoaluminium and NaCo(CO)$_4$ (ref. 110).

Then, DMPL underwent ring-opening polymerization using an appropriate metal-alkoxide catalyst to produce PHMB. The syndiotactic and atactic *cis*-PHMBs show brittle behaviour with a strain at break of only 4 and 15.7%, respectively. The isotactic *cis*-PHMB shows a strain at break larger than 100%. To obtain a PHMB sample with improved mechanical performance, a strategy of incorporating *trans* repeating units in the backbone to reduce the crystallinity was developed, and an atactic PHMB with 90% *cis* repeating units and $P_r = 0.54$ was obtained. This polymer displays a high $T_m$ (160, 173 °C) and thermal stability ($T_{d,5\%}$ = 297 °C), a strain at break of 446% and a Young's modulus of 0.467 GPa, which is similar to the mechanical performance of isotactic PP.

In summary, in PHAs, the steric interactions that arise from bulky groups in the α-position minimize the energy of the *trans*-planar conformation of the chains. This allows the chains to be packed in the crystalline form, even with a random configuration distribution of the methyl group in the β-position.

## Conclusions and outlook

This categorization and analysis of the origin and reasons for the crystallization of stereoirregular polymers has enabled us to highlight examples of polymers that show tacticity-independent crystallization and to describe the different factors that lead to crystallization in various cases. Depending on the various classes of polymers—apolar polyolefins, polar vinyl monomers, polythioesters or PHAs—diverse factors can induce crystalline order, despite the presence of configurational disorder. These include specific secondary interactions such as hydrogen bonds and dipolar attractions that can stabilize defective crystallizable conformations, conformational flexibility in the case of polymers containing cycloalkane units in the backbone, where the intrinsic conformational freedom of five- and six-membered rings is transferred to the polymer backbone, and steric interactions that arise from bulky groups installed at the specific positions of polymer backbones. Although polymers with different tacticities can crystallize, their melting temperatures and degrees of crystallinity are still a function of chain regio- and stereoregularity.

These examples of tacticity-independent crystallization are a clear manifestation of a more general concept that is the basis of modern polymer crystallography. Crystallization in polymers is a complex process that is compatible with the absence of true three-dimensional long-range order. Therefore, structural disorder in polymer crystals is more common than previously considered[14,22]. Unlike metals, the concept of crystallization in polymers is complex and far from the ideal periodic array of identical motifs that implies a complete three-dimensional long-range order of all atoms. The disorder in some polymers can be described as a structural feature and often does not prevent crystallization. The disorder in the configuration of successive repeating monomer units along a polymer chain, when tolerated, can yield tacticity-independent crystallization, bringing about remarkable ease in the synthesis of semicrystalline polymers with improved mechanical properties but without the stringent requirement of control over the polymerization stereochemistry using specifically designed or rather complex stereoselective catalysts.

A fascinating future direction is to synergistically couple the synthetic ease of atactic polymers with the properties and advantages that can be derived from the tacticity-independent crystallization described here—for example, combining the polymer's high mechanical strength and thermal, solvent or gas-permeation resistance, due to the presence of (often tempered or smaller) crystalline domains, with the enhanced ductility (thus toughness) and transparency that is due to the presence of configurational disorder, thereby overcoming the structure/crystallization–property trade-offs that persist in conventional stereoregularity-driven semicrystalline polymers. Another direction is to explore other chemical structure motifs that could yield tacticity-independent crystallization as well as non-structure-based, engineering- or processing-focused methods such as chain stretching and the quenching of atactic polymers aided by crystallization-inducing external reagents.

## References


1. Carter, B. C. & Norton, M. G. in *Ceramic Materials: Science and Engineering* 71–86 (Springer, 2007).
2. Wegst, U. G. K., Bai, H., Saiz, E., Tomsia, A. P. & Ritchie, R. O. Bioinspired structural materials. *Nat. Mater.* **14**, 23–36 (2015).
3. Ganewatta, M. S., Wang, Z. & Tang, C. Chemical syntheses of bioinspired and biomimetic polymers toward biobased materials. *Nat. Rev. Chem.* **5**, 753–772 (2021).
4. Hu, W.-B. Polymer features in crystallization. *Chin. J. Polym. Sci.* **40**, 545–555 (2022).
5. Lovinger, A. J. in *Phase Transitions in Polymers: The Rule of Metastable States* ix–xi (Elsevier, 2008).
6. Geyer, R., Jambeck, J. R. & Law, K. L. Production, use, and fate of all plastics ever made. *Sci. Adv.* **3**, e1700782 (2017).
7. Kundu, P. P., Biswas, J., Kim, H. & Choe, S. Influence of film preparation procedures on the crystallinity, morphology and mechanical properties of LLDPE films. *Eur. Polym. J.* **39**, 1585–1593 (2003).
8. Pantani, R. & Sorrentino, A. Influence of crystallinity on the biodegradation rate of injection-moulded poly(lactic acid) samples in controlled composting conditions. *Polym. Degrad. Stab.* **98**, 1089–1096 (2013).
9. Drieskens, M. et al. Structure versus properties relationship of poly(lactic acid). I. Effect of crystallinity on barrier properties. *J. Polym. Sci. B Polym. Phys.* **47**, 2247–2258 (2009).
10. Compañ, V., Del Castillo, L. F., Hernández, S. I., López-González, M. M. & Riande, E. Crystallinity effect on the gas transport in semi-crystalline coextruded films based on linear low density polyethylene. *J. Polym. Sci. B Polym. Phys.* **48**, 634–642 (2010).
11. Men, Y., Rieger, J. & Strobl, G. Role of the entangled amorphous network in tensile deformation of semi-crystalline polymers. *Phys. Rev. Lett.* **91**, 095502 (2003).
12. Mandelkern, L. The crystallization of flexible polymer molecules. *Chem. Rev.* **56**, 903–958 (1956).
13. De Rosa, C. & Auriemma, F. in *Handbook of Polymer Crystallization* (eds Piorkowska, E. & Rutledge, G. C.) Ch. 2 (Wiley, 2013).
14. De Rosa, C. & Auriemma, F. (eds) *Crystals and Crystallinity in Polymers: Diffraction Analysis of Ordered and Disordered Crystals* (Wiley, 2013).
15. Cavallo, D. & Müller, A. J. in Macromolecular Engineering: From Precise Synthesis to Macroscopic Materials and Applications Vol. 4 (eds Matyjaszewski, K. et al.) Ch. 44 (Wiley, 2022).
16. Jordan, E. F. Jr, Feldeisen, D. W. & Wrigley, A. N. Side-chain crystallinity. I. Heats of fusion and melting transitions on selected homopolymers having long side chains. *J. Polym. Sci. A1* **9**, 1835–1851 (1971).
17. Greenberg, S. A. & Alfrey, T. Side chain crystallization of *n*-alkyl polymethacrylates and polyacrylates. *J. Am. Chem. Soc.* **76**, 6280–6285 (1954).
18. Shi, H., Zhao, Y., Dong, X., Zhou, Y. & Wang, D. Frustrated crystallisation and hierarchical self-assembly behaviour of comb-like polymers. *Chem. Soc. Rev.* **42**, 2075–2099 (2013).
19. Kusanagi, H., Tadokoro, H. & Chatani, Y. Conformational and packing stability of crystalline polymers. VII. A method for the minimization of conformational and packing energies of crystalline polymers. *Polym. J.* **9**, 181–190 (1977).
20. Corradini, P., Napolitano, R., Petraccone, V., Pirozzi, B. & Tuzi, A. The role of intra- and intermolecular interactions in determining the conformation and mode of packing of crystalline polymers—I. Poly(*cis*-1,4-butadiene). *Eur. Polym. J.* **17**, 1217–1224 (1981).

21. Dasgupta, S., Hammond, W. B. & Goddard, W. A. Crystal structures and properties of nylon polymers from theory. *J. Am. Chem. Soc.* **118**, 12291–12301 (1996).
22. Corradini, P., Auriemma, F. & De Rosa, C. Crystals and crystallinity in polymeric materials. *Acc. Chem. Res.* **39**, 314–323 (2006).
23. Farina, M. in *Topics in Stereochemistry* Vol. 17 (eds Eliel, E. L. & Wilen, S. H.) Ch. 1 (Wiley, 1987).
24. Farina, M., Di Silvestro, G. & Sozzani, P. Hemitactic polymers. *Prog. Polym. Sci.* **16**, 219–238 (1991).
25. De Rosa, C. in *Materials-Chirality* Vol. 24 (eds Green, M. M. et al.) Ch. 2 (Wiley, 2003).
26. Coates, G. W. Precise control of polyolefin stereochemistry using single-site metal catalysts. *Chem. Rev.* **100**, 1223–1252 (2000).
27. Miri, M. J., Pritchard, B. P. & Cheng, H. N. A versatile approach for modeling and simulating the tacticity of polymers. *J. Mol. Model.* **17**, 1767–1780 (2011).
28. Natta, G. et al. Crystalline high polymers of α-olefins. *J. Am. Chem. Soc.* **77**, 1708–1710 (1955).
29. Natta, G. Une nouvelle classe de polymeres d'α-olefines ayant une régularité de structure exceptionnelle. *J. Polym. Sci.* **16**, 143–154 (1955).
30. Natta, G. in *Nobel Lectures in Chemistry 1963–1970* 27–60 (Elsevier, 1963).
31. Spassky, N., Wisniewski, M., Pluta, C. & Le Borgne, A. Highly stereoelective polymerization of *rac*-(D,L)-lactide with a chiral Schiff's base/aluminium alkoxide initiator. *Macromol. Chem. Phys.* **197**, 2627–2637 (1996).
32. Ovitt, T. M. & Coates, G. W. Stereochemistry of lactide polymerization with chiral catalysts: new opportunities for stereocontrol using polymer exchange mechanisms. *J. Am. Chem. Soc.* **124**, 1316–1326 (2002).
33. Zhong, Z., Dijkstra, P. J. & Feijen, J. Controlled and stereoselective polymerization of lactide: kinetics, selectivity, and microstructures. *J. Am. Chem. Soc.* **125**, 11291–11298 (2003).
34. Tang, X. & Chen, E. Y.-X. Chemical synthesis of perfectly isotactic and high melting bacterial poly(3-hydroxybutyrate) from bio-sourced racemic cyclic diolide. *Nat. Commun.* **9**, 2345 (2018).
35. Tang, X., Westlie, A. H., Watson, E. M. & Chen, E. Y.-X. Stereosequenced crystalline polyhydroxyalkanoates from diastereomeric monomer mixtures. *Science* **366**, 754–758 (2019).
36. Zhang, Z., Shi, C., Scoti, M., Tang, X. & Chen, E. Y.-X. Alternating isotactic polyhydroxyalkanoates via site- and stereoselective polymerization of unsymmetrical diolides. *J. Am. Chem. Soc.* **144**, 20016–20024 (2022).
37. Tubbs, R. K. Melting point and heat of fusion of poly(vinyl alcohol). *J. Polym. Sci. A* **3**, 4181–4189 (1965).
38. Juijn, J. A., Gisolf, J. H. & de Jong, W. A. Crystallinity in atactic poly(vinyl chloride). *Kolloid Z. Z. Polym.* **251**, 456–473 (1973).
39. Zhou, L. et al. Chemically circular, mechanically tough, and melt-processable polyhydroxyalkanoates. *Science* **380**, 64–69 (2023).
40. Shi, C. et al. High-performance pan-tactic polythioesters with intrinsic crystallinity and chemical recyclability. *Sci. Adv.* **6**, eabc0495 (2020).
41. Hubbard, R. E. & Kamran Haider, M. Hydrogen bonds in proteins: role and strength. In *Encyclopedia of Life Sciences* (Wiley, 2010).
42. Sherrington, D. C. & Taskinen, K. A. Self-assembly in synthetic macromolecular systems via multiple hydrogen bonding interactions. *Chem. Soc. Rev.* **30**, 83–93 (2001).
43. Aslam, M., Kalyar, M. A. & Raza, Z. A. Polyvinyl alcohol: a review of research status and use of polyvinyl alcohol based nanocomposites. *Polym. Eng. Sci.* **58**, 2119–2132 (2018).
44. Wong, D. & Parasrampuria, J. Polyvinyl alcohol. *Anal. Profiles Drug Subst. Excip.* **24**, 397–441 (1996).
45. Moritani, T., Kuruma, I., Shibatani, K. & Fujiwara, Y. Tacticity of poly(vinyl alcohol) studied by nuclear magnetic resonance of hydroxyl protons. *Macromolecules* **5**, 577–580 (1972).
46. Mooney, R. C. L. An X-ray study of the structure of polyvinyl vlcohol. *J. Am. Chem. Soc.* **63**, 2828–2832 (1941).
47. Bunn, C. W. Crystal structure of polyvinyl alcohol. *Nature* **161**, 929–930 (1948).
48. Tashiro, K., Kusaka, K., Yamamoto, H. & Hanesaka, M. Introduction of disorder in the crystal structures of atactic poly(vinyl alcohol) and its iodine complex to solve a dilemma between X-ray and neutron diffraction data analyses. *Macromolecules* **53**, 6656–6671 (2020).
49. Cazón, P., Vázquez, M. & Velázquez, G. Regenerated cellulose films with chitosan and polyvinyl alcohol: effect of the moisture content on the barrier, mechanical and optical properties. *Carbohydr. Polym.* **236**, 116031 (2020).
50. Mokwena, K. K. & Tang, J. Ethylene vinyl alcohol: a review of barrier properties for packaging shelf stable foods. *Crit. Rev. Food Sci. Nutr.* **52**, 640–650 (2012).
51. Ogba, O. M., Warner, N. C., O'Leary, D. J. & Grubbs, R. H. Recent advances in ruthenium-based olefin metathesis. *Chem. Soc. Rev.* **47**, 4510–4544 (2018).
52. da Silva, L. C., Rojas, G., Schulz, M. D. & Wagener, K. B. Acyclic diene metathesis polymerization: history, methods and applications. *Prog. Polym. Sci.* **69**, 79–107 (2017).
53. Mutlu, H., de Espinosa, L. M. & Meier, M. A. R. Acyclic diene metathesis: a versatile tool for the construction of defined polymer architectures. *Chem. Soc. Rev.* **40**, 1404–1445 (2011).
54. Guillory, G. A., Marxsen, S. F., Alamo, R. G. & Kennemur, J. G. Precise isotactic or atactic pendant alcohols on a polyethylene backbone at every fifth carbon: synthesis, crystallization, and thermal properties. *Macromolecules* **55**, 6841–6851 (2022).
55. Tashiro, K., Guillory, G. A., Marxsen, S. F., Kennemur, J. G. & Alamo, R. G. Crystal structures of isotactic and atactic poly(1-pentamethylene alcohol). *Macromolecules* **56**, 5993–6002 (2023).
56. Dingwell, C. E. & Hillmyer, M. A. Regiospecific poly(ethylene-co-vinyl alcohol) by ROMP of 3-acetoxycyclooctene and postpolymerization modification for barrier material applications. *ACS Appl. Polym. Mater.* **5**, 1828–1836 (2023).
57. Dingwell, C. E. & Hillmyer, M. A. Regio- and stereoregular EVOH copolymers from ROMP as designer barrier materials. *ACS Polym. Au* **4**, 208–213 (2024).
58. Zhang, J., Matta, M. E., Martinez, H. & Hillmyer, M. A. Precision vinyl acetate/ethylene (VAE) copolymers by ROMP of acetoxy-substituted cyclic alkenes. *Macromolecules* **46**, 2535–2543 (2013).
59. Endo, K. Synthesis and structure of poly(vinyl chloride). *Prog. Polym. Sci.* **27**, 2021–2054 (2002).
60. Saeki, Y. & Emura, T. Technical progresses for PVC production. *Prog. Polym. Sci.* **27**, 2055–2131 (2002).
61. Natta, G. & Corradini, P. The structure of crystalline 1,2-polybutadiene and of other "syndyotactic polymers". *J. Polym. Sci.* **20**, 251–266 (1956).
62. Hobson, R. J. & Windle, A. H. Crystallization and shape emulation in atactic poly(vinyl chloride) and polyacrylonitrile. *Polymer* **34**, 3582–3596 (1993).
63. Wenig, W. The microstructure of poly(vinyl chloride) as revealed by x-ray and light scattering. *J. Polym. Sci. Polym. Phys. Ed.* **16**, 1635–1649 (1978).
64. Gilbert, M. Crystallinity in poly(vinyl chloride). *J. Macromol. Sci. C Polym. Rev.* **34**, 77–135 (1994).
65. Mijangos, C., Calafel, I. & Santamaría, A. Poly(vinyl chloride), a historical polymer still evolving. *Polymer* **266**, 125610 (2023).

66. Beevers, R. B. The physical properties of polyacrylonitrile and its copolymers. *J. Polym. Sci. Macromol. Rev.* **3**, 113–254 (1968).
67. Vatanpour, V., Pasaoglu, M. E., Kose-Mutlu, B. & Koyuncu, I. Polyacrylonitrile in the preparation of separation membranes: a review. *Ind. Eng. Chem. Res.* **62**, 6537–6558 (2023).
68. Karp, E. M. et al. Renewable acrylonitrile production. *Science* **358**, 1307–1310 (2017).
69. Kamide, K., Yamazaki, H., Okajima, K. & Hikichi, H. Stereoregiilarity of polyacrylonitrile by high resolution $^{13}$C NMR analysis. *Polym. J.* **17**, 1233–1239 (1985).
70. Kamide, K., Yamazaki, H., Okajima, K. & Hikichi, K. Pentad tacticity of polyacrylonitrile polymerized by γ-ray irradiation on urea–acrylonitrile canal complex at −78 °C. *Polym. J.* **17**, 1291–1295 (1985).
71. Hobson, R. J. & Windle, A. H. Crystalline structure of atactic polyacrylonitrile. *Macromolecules* **26**, 6903–6907 (1993).
72. Liu, X. D. & Ruland, W. X-ray studies on the structure of polyacrylonitrile fibers. *Macromolecules* **26**, 3030–3036 (1993).
73. Rizzo, P., Auriemma, F., Guerra, G., Petraccone, V. & Corradini, P. Conformational disorder in the pseudohexagonal form of atactic polyacrylonitrile. *Macromolecules* **29**, 8852–8861 (1996).
74. Auriemma, F., De Rosa, C. & Corradini, P. in *Interphases and Mesophases in Polymer Crystallization II* (ed. Allegra, G.) 1–74 (Springer, 2005).
75. Kaji, H. & Schmidt-Rohr, K. Conformation and dynamics of atactic poly(acrylonitrile). 1. *Trans*/*gauche* ratio from double-quantum solid-state $^{13}$C NMR of the methylene groups. *Macromolecules* **33**, 5169–5180 (2000).
76. Kaji, H. & Schmidt-Rohr, K. Conformation and dynamics of atactic poly(acrylonitrile). 2. Torsion angle distributions in meso dyads from two-dimensional solid-state double-quantum $^{13}$C NMR. *Macromolecules* **34**, 7368–7381 (2001).
77. Kaji, H. & Schmidt-Rohr, K. Conformation and dynamics of atactic poly(acrylonitrile). 3. Characterization of local structure by two-dimensional $^{2}$H–$^{13}$C solid-state NMR. *Macromolecules* **34**, 7382–7391 (2001).
78. Rizzo, P., Guerra, G. & Auriemma, F. Thermal transitions of polyacrylonitrile fibers. *Macromolecules* **29**, 1830–1832 (1996).
79. Nataraj, S. K., Yang, K. S. & Aminabhavi, T. M. Polyacrylonitrile-based nanofibers—a state-of-the-art review. *Prog. Polym. Sci.* **37**, 487–513 (2012).
80. Yamane, A. et al. Development of high ductility and tensile properties upon two-stage draw of ultrahigh molecular weight poly(acrylonitrile). *Macromolecules* **30**, 4170–4178 (1997).
81. Kafle, N. et al. Roles of conformational flexibility in the crystallization of stereoirregular polymers. *Macromolecules* **54**, 5705–5718 (2021).
82. Torrisi, A. et al. Solid phases of cyclopentane: combined experimental and simulation study. *J. Phys. Chem. B* **112**, 3746–3758 (2008).
83. Rams-Baron, M. et al. in *Amorphous Drugs: Benefits and Challenges* 9–39 (Springer, 2018).
84. Mack, J. W. & Torchia, D. A. A deuteron NMR study of the molecular dynamics of solid cyclopentane. *J. Phys. Chem.* **95**, 4207–4213 (1991).
85. Ruiz de Ballesteros, O., Cavallo, L., Auriemma, F. & Guerra, G. Conformational analysis of poly(methylene-1,3-cyclopentylene) and chain conformation in the crystalline phase. *Macromolecules* **28**, 7355–7362 (1995).
86. Kilpatrick, J. E., Pitzer, K. S. & Spitzer, R. The thermodynamics and molecular structure of cyclopentane. *J. Am. Chem. Soc.* **69**, 2483–2488 (1947).
87. Cui, W., Li, F. & Allinger, N. L. Simulation of conformational dynamics with the MM3 force field: the pseudorotation of cyclopentane. *J. Am. Chem. Soc.* **115**, 2943–2951 (1993).
88. Nakama, Y., Hayano, S. & Tashiro, K. Influence of tacticity on the crystal structures of hydrogenated ring-opened poly(norbornene) s. *Macromolecules* **54**, 8122–8134 (2021).
89. Lee, L.-B. W. & Register, R. A. Hydrogenated ring-opened polynorbornene: a highly crystalline atactic polymer. *Macromolecules* **38**, 1216–1222 (2005).
90. Bishop, J. P. & Register, R. A. The crystal–crystal transition in hydrogenated ring-opened polynorbornenes: tacticity, crystal thickening, and alignment. *J. Polym. Sci. B Polym. Phys.* **49**, 68–79 (2011).
91. Klein, J. P. & Register, R. A. Tuning the phase behavior of semi-crystalline hydrogenated polynorbornene via epimerization. *J. Polym. Sci. B Polym. Phys.* **57**, 1188–1195 (2019).
92. Nakama, Y., Hayano, S. & Tashiro, K. X-ray-analyzed structural changes in the crystal phase transitions of hydrogenated ring-opened poly(norbornene)s with different stereoregularities. *Macromolecules* **57**, 1677–1687 (2024).
93. Ruiz de Ballesteros, O. et al. Thermal and structural characterization of poly(methylene-1,3-cyclopentane) samples of different microstructures. *Macromolecules* **28**, 2383–2388 (1995).
94. Marvel, C. S. & Stille, J. K. Intermolecular–intramolecular polymerization of α-diolefins by metal alkyl coöordination catalysts. *J. Am. Chem. Soc.* **80**, 1740–1744 (1958).
95. Marvel, C. S. & Garrison, W. E. Jr. Polymerization of higher α-diolefins with metal alkyl coordination catalysts. *J. Am. Chem. Soc.* **81**, 4737–4744 (1959).
96. Makowski, H. S., Shim, B. K. C. & Wilchinsky, Z. W. 1,5-Hexadiene polymers. I. Structure and properties of poly-1,5-hexadiene. *J. Polym. Sci. A* **2**, 1549–1566 (1964).
97. Cheng, H. N. & Khasat, N. P. $^{13}$C-NMR characterization of poly(1,5-hexadiene). *J. Appl. Polym. Sci.* **35**, 825–829 (1988).
98. Resconi, L. & Waymouth, R. M. Diastereoselectivity in the homogeneous cyclopolymerization of 1,5-hexadiene. *J. Am. Chem. Soc.* **112**, 4953–4954 (1990).
99. Resconi, L., Coates, G. W., Mogstad, A. & Waymouth, R. M. Stereospecific cyclopolymerization with group 4 metallocenes. *J. Macromol. Sci. A Chem.* **28**, 1225–1234 (1991).
100. Cavallo, L., Guerra, G., Corradini, P., Resconi, L. & Waymouth, R. M. Model catalytic sites for olefin polymerization and diastereo-selectivity in the cyclopolymerization of 1,5-hexadiene. *Macromolecules* **26**, 260–267 (1993).
101. Coates, G. W. & Waymouth, R. M. Enantioselective cyclopolymeri-zation of 1,5-hexadiene catalyzed by chiral zirconocenes: a novel strategy for the synthesis of optically active polymers with chirality in the main chain. *J. Am. Chem. Soc.* **115**, 91–98 (1993).
102. Okada, T., Takeuchi, D., Shishido, A., Ikeda, T. & Osakada, K. Isomerization polymerization of 4-alkylcyclopentenes catalyzed by Pd complexes: hydrocarbon polymers with isotactic-type stereochemistry and liquid-crystalline properties. *J. Am. Chem. Soc.* **131**, 10852–10853 (2009).
103. Naga, N., Tsubooka, M., Sone, M., Tashiro, K. & Imanishi, Y. Crystalline structure of polyethylene containing 1,2- or 1,3-disubstituted cyclopentane units in the main chain. *Macromolecules* **35**, 9999–10003 (2002).
104. Van Zee, N. J. & Coates, G. W. Alternating copolymerization of dihydrocoumarin and epoxides catalyzed by chromium salen complexes: a new route to functional polyesters. *Chem. Commun.* **50**, 6322–6325 (2014).
105. Shi, C., Reilly, L. T. & Chen, E. Y.-X. Hybrid monomer design synergizing property trade-offs in developing polymers for circularity and performance. *Angew. Chem. Int. Ed.* **62**, e202301850 (2023).
106. Hu, Z. et al. Terpenoid-based high-performance polyester with tacticity-independent crystallinity and chemical circularity. *Chem.* **10**, 3040–3054 (2024).

107. Huang, H.-Y. et al. Spiro-salen catalysts enable the chemical synthesis of stereoregular polyhydroxyalkanoates. *Nat. Catal.* **6**, 720–728 (2023).
108. Phongtamrug, S. & Tashiro, K. X-ray crystal structure analysis of poly(3-hydroxybutyrate) β-form and the proposition of a mechanism of the stress-induced α-to-β phase transition. *Macromolecules* **52**, 2995–3009 (2019).
109. Scoti, M., Zhou, L., Chen, E. Y.-X. & De Rosa, C. Crystal structure of atactic and isotactic poly(3-hydroxy-2,2-dimethylbutyrate): a chemically recyclable poly(hydroxyalkanoate) with tacticity-independent crystallinity. *Macromolecules* **57**, 4357–4373 (2024).
110. Zhou, Z., LaPointe, A. M. & Coates, G. W. Atactic, isotactic, and syndiotactic methylated polyhydroxybutyrates: an unexpected series of isomorphic polymers. *J. Am. Chem. Soc.* **145**, 25983–25988 (2023).

## Acknowledgements

L.S., A.S., M.X., H.S. and A.J.M. acknowledge support from the following projects: the María de Maeztu Excellence Unit CEX2023-001303-M funded by MCIN/AEI/10.13039/501100011033; PID2023-149734NB-C22 funded by MCIN/AEI/10.13039/501100011033, TED2021-129852B-C22 funded by MCIN/AEI/10.13039/501100011033 and PID2022-138199NB-I00 funded by MCIN/AEI/10.13039/501100011033; the Basque Country Government, GC IT 1667-22; and Universidad del País Vasco UPV/EHU, EHU-N24/54. M.X. acknowledges the Gipuzkoa Fellows Programme from the Provincial Council of Gipuzkoa, grant G75067454. L.S. thanks the Gipuzkoa Fellows Programme from the Provincial Council of Gipuzkoa, grant 2024-FELL-000010. L.S. also acknowledges the fellowship from the "la Caixa" Foundation (ID 100010434) (code B006525). M.S. and C.D.R. acknowledge financial support from the project PRIN-PNRR 2022 (grant no. P2022N9T7X) of the Ministry of University of Italy "Polymers of tunable molecular structure and properties from bio-renewable sources designed for a complete chemical recycling to monomers (Re-Tune)". E.Y.-X.C. acknowledges support by the US National Science Foundation (NSF-2305058). The work by C.S. was supported by the BOTTLE Consortium funded by the US Department of Energy via the National Laboratory of the Rockies under Contract DE-AC36-08GO28308. The funders had no role in the study design, data collection and analysis, decision to publish or preparation of the manuscript.

## Author contributions

All authors contributed to discussions and the writing of the manuscript.

## Competing interests

The authors declare no competing interests.

## Additional information

**Correspondence and requests for materials** should be addressed to Claudio De Rosa, Eugene Y.-X. Chen, Haritz Sardon or Alejandro J. Müller.

**Peer review information** *Nature Chemistry* thanks Wenbing Hu and Toshikazu Miyoshi for their contribution to the peer review of this work.